Title	In-situ observations of nanoscale effects in germanium nanowire growth with ternary eutectic alloys
Authors	Biswas, Subhajit;O'Regan, Colm;Morris, Michael A.;Holmes, Justin D.
Publication date	2014-09-05
Original Citation	BISWAS, S., O'REGAN, C., MORRIS, M. A. & HOLMES, J. D. 2015. In-situ Observations of Nanoscale Effects in Germanium Nanowire Growth with Ternary Eutectic Alloys. Small, 11, 103-111. http://dx.doi.org/10.1002/smll.201401240
Type of publication	Article (peer-reviewed)
Link to publisher's version	http://onlinelibrary.wiley.com/journal/10.1002/(ISSN)1613-6829 - 10.1002/smll.201401240
Rights	© 2014 Wiley-VCH Verlag GmbH & Co. KGaA, Weinheim. This is the accepted version of the following article: Biswas, S., O'Regan, C., Morris, M. A. and Holmes, J. D. (2015), In-situ Observations of Nanoscale Effects in Germanium Nanowire Growth with Ternary Eutectic Alloys. Small, 11: 103–111. doi:10.1002/smll.201401240, which has been published in final form at http://dx.doi.org/10.1002/smll.201401240.
Download date	2025-07-31 20:14:24
Item downloaded from	https://hdl.handle.net/10468/2242

In-situ Observations of Nanoscale Effects in Germanium Nanowire Growth with Ternary Eutectic Alloys

Subhajit Biswas, Colm O'Regan, Michael A. Morris and Justin D. Holmes[*]

Materials Chemistry & Analysis Group, Department of Chemistry and the Tyndall National Institute, University College Cork, Cork, Ireland. Centre for Research on Adaptive Nanostructures and Nanodevices (CRANN), Trinity College Dublin, Dublin 2, Ireland.

[*] Corresponding Author: Prof. Justin D. Holmes

Tel: +353(0)21 4903608

Fax: +353(0)21 4274097

E-mail: j.holmes@ucc.ie

Abstract: Vapour-liquid-solid (VLS) techniques are popular routes for the scalable synthesis of semiconductor nanowires. In this article, in-situ electron microscopy is used to correlate the equilibrium content of ternary ($Au_{0.75}Ag_{0.25}$-Ge and $Au_{0.65}Ag_{0.35}$-Ge) metastable alloys with the kinetics, thermodynamics and diameter of Ge nanowires grown via a VLS mechanism. The shape and geometry of the heterogeneous interfaces between the liquid eutectic and solid Ge nanowires varies as a function of nanowire diameter and eutectic alloy composition. The behaviour of the faceted heterogeneous liquid-solid interface links with the growth kinetics of the nanowires, where the truncated facets at the solid nanowire-liquid catalyst drop contact line lengthens for faster nanowire growth kinetics. Pronounced diameter dependent growth kinetics, as inferred from liquid-solid interfacial behaviour, is apparent for the synthesised nanowires. Direct in-situ microscopy observations facilitates the comparison between the nanowire growth behaviour from ternary (Au-Ag-Ge) and binary (Au-Ge) eutectic systems.

2

1. Introduction

Three phase vapour-liquid-solid (VLS) growth processes enable the synthesis of semiconductor nanowires with controllable structure and composition, paving the way for their application in nanoscale electronics, photonics and sensing devices.[1-8] Gold (Au) is the most commonly used growth promoter for the VLS growth of Ge or Si nanowires; forming Au-Ge and Au-Si binary eutectic alloy respectively during one-dimensional (1-D) crystal growth. The composition of the liquid metal-semiconductor binary eutectic alloy (Au-Ge or Au-Si), governs the supersaturation, or driving force[9], in a layer-by-layer 1-D crystal growth process[10], and hence nanowire VLS-growth kinetics. Equilibrium phase diagrams, mainly the liquidus curves (metal and semiconductor liquidus), provide information about the composition of eutectics at different temperatures during nanowire growth. A shift in the liquidus curve, *i.e.* the equilibrium composition of the eutectic alloy, alters the supersaturation of the catalyst seeds which subsequently influences the kinetics of nanowire growth; favouring faster crystallisation rates at the TPB at high supersaturation values.[11, 12] A shift in the liquidus of Au-Ge (or Au-Si) binary alloy can therefore be achieved by incorporating an external metal (foreign) element into the metal-semiconductor eutectic.[13] For example, incorporation of Ag ($\leq$ 25 at%) leads to an altered eutectic equilibrium concentration of Ge in the liquid phase and hence a change in the supersaturation and nanowire growth kinetics.[14] Determination of the Ge-liquidus from Ge equilibrium concentrations of nanoscale ternary eutectic systems (Au-Ag-Ge), will enable interpretation of supersaturation and hence nanowire growth kinetics (as this depends on supersaturation) from ternary eutectic systems, compared to binary systems (Au-Ge). In-situ electron microscopy experiments provide a feasible way to calculate equilibrium concentrations of Ge [15] at elevated temperatures in metastable eutectic alloys, permitting determination of Ge-liquidus curves for different sized nanoscale binary and ternary systems. A modified phase

diagram has been shown for nanoscale systems (especially for binary Au-Ge), compared to their bulk counterparts, due to the influence of capillary forces and stress at the nanoscale.[15-17]

Apart from the Ge concentration in the eutectic volume, the behaviour of the triple phase boundary (TPB) at the nanowire-liquid metal interface provides an understanding of growth phenomenon at an atomic level.[18-24] For example, interfacial energies and capillary forces during steady-state nanowire growth determine the dynamics of the seed droplet at the tip of a nanowire, *e.g.* influencing the pinning of the droplet seed at the nanowire sidewall facets.[20, 22] Also, the capillary-related wetting behaviour of a non-planar catalyst-nanowire interface can be associated with the nucleation barrier of a 2D-island at the TPB.[18] The position and shape of the droplet at a nanowire tip determines the facet dynamics and hence nominal crystal growth. In-situ observation of liquid-solid interfaces at nanowire growth temperatures between ~400-500 °C[14, 25-27], provide the opportunity to correlate liquid-solid interfacial behaviour to nanowire growth kinetics.[22, 28] Thus observation of the characteristics of the liquid-solid interfaces for ternary (Au-Ag-Ge) and binary alloys (Au-Ge) at nanowire growth temperatures enables comparison of nanowire growth kinetics for binary and ternary alloy systems.

However, direct evaluation of eutectic droplet shapes and the triple phase contact line at the liquid-solid-vapour interface during nanowire growth is highly demanding. High temperature in-situ electron microscopy experiments have provided the opportunity to replicate and visualise nanowire growth over a range of temperatures, allowing catalyst-nanowire interface dynamics to be investigated.[19, 29, 30] In this article, the nanoscale behaviour associated with the growth of Ge nanowires from ternary eutectic (Au-Ag-Ge) alloys, assuming an equilibrium growth scenario, is explored via post-growth high temperature in-situ electron microscopy. Specifically, the shape of the liquid droplet and the

4

liquid (seed)-solid (nanowire) contact line are related to the equilibrium concentration and the supersaturation of Ge in the catalyst drop. Additionally, a correlation between the nanowire growth kinetics and the dynamics at the catalyst seed-nanowire interface is investigated for eutectic systems of different dimensions and compositions.

2. Results and Discussion

The first issue to consider is the equilibrium concentration of Ge and the projection of Ge-liquidus for ternary eutectic systems. Linear and quadratic dependences of nanowire growth rates on $\Delta\mu$ have been reported with VLS models, where the rate limiting step involves nucleation and growth of 2D-islands at the seed-nanowire interface.[9, 31-33] The magnitude of the concentration (C) of the growth species in a solid or liquid solution can be written in terms of the supersaturation ($\Delta\mu$), the thermal energy of the system (kT) and the equilibrium concentration (C_e) for a bulk system as $\Delta\mu = kT\ln(C/C_e)$, where the equilibrium concentration signifies the concentration above which a eutectic rejects its excess Ge content. Au-Ge is the most popular binary eutectic system investigated for the VLS growth of Ge nanowires, due to the low eutectic melting temperature and high solubility of Ge. A deviation in the Au-Ge phase diagram, mainly the Ge-liquidus, *i.e.* the equilibrium concentration, is expected upon the inclusion of a small amount of Ag into the binary eutectic[13], thus influencing $\Delta\mu$ and the kinetics of VLS-nanowire growth.[13, 14]

2.1 Nanoscale shift in Ge-liquidus and the resulting effect on supersaturation

Apart from the deviation in the Ge-liquidus with the incorporation of Ag into the Au-Ge eutectic, a divergence in the liquidus is also expected due to nanosize effects, resulting from an enhanced surface contribution. The change in the equilibrium concentration of a

nanoscale eutectic droplet (C_{nano}) of a given diameter (d), compared to its bulk counterpart (C_{bulk}), is predicted according to: $C_{nano} = C_{bulk} \exp(\kappa 4\Omega\gamma/dkT)$, where κ is a shape constant at a certain temperature (from Henry's law: $P_i = \kappa C_i$), Ω is the atomic volume of the liquid and γ is the surface energy.[11] In this study ternary eutectic alloys ($Au_{0.75}Ag_{0.25}$-Ge and $Au_{0.65}Ag_{0.35}$-Ge) were compared with a conventional binary eutectic system (Au-Ge) via nanowire post growth in-situ TEM annealing experiments (Inset in **Figure 1** shows EDX compositional analysis at the tips of the Ge nanowires at room temperature). The behaviour of binary and ternary eutectic alloy droplets of different dimensions, at the tips of the Ge nanowires, was recorded at various temperatures (see **Figure S1** in the Supporting Information). Au and AuAg-seeded Ge nanowires were grown using a liquid-injection chemical vapour deposition technique (see Supporting Information for details about nanowire synthesis). Only [111]-directed nanowires with no evidence of carbon or any amorphous outer shells (at temperature > 300 ℃) at the nanowire and metal tip surfaces were considered for post-growth experiments to omit any surface energy-related effects with different faceted nanowires (**Figure 1 and S2** in Supporting Information shows transmission electron microscopy (TEM) images of [111] oriented Ge nanowires) and possible changes to interfacial surface energies resulting from carbon shells. Nanowires grown with ternary drops were mostly single crystalline in nature, with a minimal number (around 5-10 % of total nanowires) of nanowires containing twinning and stacking faults or kinks (**Figure 1** shows TEM and SEM images of the Ge nanowires).[14] The composition and diameter-dependent melting of metal seeds at the tips of Ge nanowires were determined from in-situ TEM experiments; with relatively higher melting temperatures (~430-440 ℃) noted for alloys with a higher Ag content and larger dimensions. TEM images depicted in **Figures S1 and S3** (in Supporting Information) and the selected area electron diffraction (SAED)

patterns recorded from seed-nanowire interface areas (**Figure S3**) confirms the melting of the seeds at the tips of the nanowires with no observed diffraction spots, corresponding to melted metallic components, at elevated temperatures. The increase in the melting point of the eutectic alloys with increasing Ag content is due to the elevation of the bulk eutectic temperature for a Ag-Au-Ge system compared to a Au-Ge system.[13] Although a large undercooling, relative to the bulk eutectic, was previously reported for Au-Ge binary alloys owing to Ge supersaturation at lower temperatures for nanoscale systems[34], only a small depression (~5-25 ºC) in the eutectic temperature was observed for eutectic droplets investigated in this study with diameters between 25-70 nm. The lowering of the eutectic temperature for nanosized systems is associated with capillary effects and an increase in the Gibbs energy for nanoscale binary and ternary systems.[35] Capillary effects, often represented by the Gibbs-Thomson pressure, and which are proportional to the product of the surface curvature and surface energy, increase the Gibbs energy of the nanoparticle catalyst and the nanowire relative to their bulk values. For nanoscale binary and ternary eutectic systems, the total Gibbs energy becomes very significant at high surface energies, resulting in a lowering of the eutectic temperature for nanosize objects.[36]

A further increase in the in-situ annealing temperature away from the eutectic point results in a gradual increase in the volume of the alloy droplet, due to an expansion of the interface between the liquid alloy and solid nanowire (**Figure S1** in Supporting Information). The change in the volume of the liquid alloy droplets, due to Ge uptake from the nanowire, as a function of temperature for the different eutectic systems (Au-Ge and Au-Ag-Ge) was measured, allowing the equilibrium compositions of Ge in the various eutectic melts to be determined.[16] Drop-volume measurements ($V(T)$) of the liquid spherical cap (the dark, contrasted Au-Ge and Au-Ag-Ge tips of the nanowires shown in **Figure S1**) on top of the

7

cylindrical nanowires provided an estimate of the equilibrium Ge concentration (N_{Ge}) according to $N_{Ge}v_{Ge} = V(T) - \Sigma\ N_i v_i$, where N_i is the number of metal atoms of eutectic components in the drop and v_i and v_{Ge} are the atomic volumes of the metal components and Ge respectively (see Supporting Information for detailed discussion on the calculation of equilibrium concentrations).[15] Each Ge-liquidus in the semiconductor-rich side of the phase diagram were evaluated from the equilibrium Ge concentrations (N_{Ge}) in the metastable binary and ternary eutectics (**Figure 2**). Ge-liquidus curves for binary and ternary systems over the temperature range of 360-500 ºC were determined, representing the most relevant temperatures for VLS growth of Ge nanowires.[25, 37-39] **Figure 2(a)** compares the calculated Ge-liquidus curves for ternary Au-Ag-Ge alloy systems with the Ge-liquidus of the bulk (green line) and nanoscale (for various radial dimensions within 24-65 nm) of Au-Ge systems. For a certain composition of metal (Au or AuAg) in a eutectic system and at a certain temperature, the Ge-liquidus shifts towards a higher Ge content with decreasing diameter due to nanosize effects, implying enhanced eutectic melting of the smaller metastable eutectic alloys, which contain higher Ge concentrations than larger diameter eutectics. With the inclusion of Ag in the Au-Ge eutectic alloys, the liquidus curves moves towards a lower Ge concentration compared to the Au-Ge liquidus, with the largest shift observed for the $Au_{0.65}Ag_{0.35}$-Ge system. The shift in the liquidus curves, *i.e.* equilibrium concentrations, directly affects the Ge supersaturation ($\Delta\mu$); with high $\Delta\mu$ values expected at low equilibrium concentrations (C_e)[14], according to the equation: $\Delta\mu = kT\ln\left(C/C_e\right)$. Experimental observations of the Ge-liquidus for different sized binary and ternary eutectic alloys were verified through a theoretical fit based on the Gibbs-Thompson equation.[11] The diameter dependent Ge content at 460 and 480 °C in the Au-Ge, $Au_{0.75}Ag_{0.25}$-Ge, and $Au_{0.65}Ag_{0.35}$-Ge eutectic alloys for different nanowire diameters are shown in **Figure 2(b)**. Experimental data agrees well with the simulated curves (dashed lines) for all three of the

eutectic alloys considered. A three atomic percent error (in the Y-axis) is included with the calculated values of Ge equilibrium concentrations. This incorporated error in the equilibrium concentration accounts for the inaccuracies in calculating the volume expansion (due to deformation from spherical cap shape) of a eutectic drop due to Ge uptake. The little discrepancies between the experimental and simulated plots may be due to the difference between simulating spherical particle tips and calculating the Ge concentration from actual hemispherical seeds.[40] An upward trend in the Ge equilibrium concentration as a function of decreasing nanowire diameter was clearly evident for all of the eutectic systems studied, in agreement with the Gibbs-Thompson effect, *i.e.* the supersaturation ($\Delta\mu$) becomes diameter (*d*) dependent according to: $\Delta\mu = \Delta\mu_0 - 4\Omega\alpha/d$, where $\Delta\mu_0$ is the supersaturation at a plane boundary ($d \rightarrow \infty$), Ω is the atomic volume of the liquid and α is the surface energy. The change in the Ge-equilibrium concentration in the eutectic alloys at different dimensions and compositions can be directly related to the supersaturation and nanowire growth kinetics, as reported in our previous report and other publications.[9, 14, 33, 41]

2.2 Catalyst-nanowire interface characteristics

Equilibrium compositions of a eutectic drop determine the interfacial dynamics between a liquid catalyst and a nanowire through the balance of interfacial forces at the TPB. Interfacial dynamics at the TPB also act as an indicative measure of the kinetics of nanowire growth.[20, 22, 28] The balance of interfacial forces (vapour-liquid (γ_{vl}), solid-liquid (γ_{sl}) and vapour-solid (γ_{vs}) surface energies) determines the equilibrium shape of the solid nanowire-liquid catalyst interface at steady state. For an equilibrated liquid drop-nanowire system, often a flat interface between the liquid droplet and semiconductor nanowire, with sharp corners at the TPB contact line, is observed.[32, 42] However, recent theoretical and in-situ experimental

studies have demonstrated a faceted interface at the TPB with truncation at the corner of the TPB contact lines.[20, 21, 23, 28, 32, 42] Probable structures of liquid-solid interfaces, *i.e.* flat and truncated interfaces with different facet lengths at the TPB are shown in **Figure S4**. The Young's balance of forces along the liquid-solid and vapour-solid interfaces account for stepped structures, *i.e.* facets, at the corner of the TPB contact line for <111> directed nanowires. The truncating facets mainly consist of the {113} family of planes at the corner of the TPB line. For the liquid-solid interface of liquid metal alloys with solid Ge <111> semiconductor nanowires, {111} centre facets dominate the length of the TPB contact line with {113} truncated facets extending for a few nanometers (< 10 nm) at the edges (**Figure 3(a)**). The faceted shape of the liquid-solid interface observed in our case agrees well with the theoretical observation of the TPB morphology during VLS nanowire growth[22, 43], taking into account the balance of Young's forces at the TPB. Our observations of the truncated liquid-solid interface with {111} centre facets at the TPB for Au-Ge and Au-Ag-Ge systems also agrees well with the equilibrium Wulff shape for a diamond cubic (DC) crystal of Ge; for a equilibrated liquid drop-nanowire system.[22, 44] Schematics of faceted catalyst drop-nanowire interfaces with different surface forces and wetting angles are shown in **Figure 3(a)**, where the relative degree of truncation represents a different scale of atomic order, or roughness, at the TPB.[20] The TEM image of a AuGe liquid drop-Ge nanowire system (pictured at 420 ℃) and the SAED pattern recorded at the liquid-solid interface confirms the multi-faceted interface with central {111} planes surrounded by {113} faceted segments at the periphery (**Figure 3(a)**).[16] As Ge uptake from the nanowires, through a time dependent diffusion process, can change the interfacial dynamics (**Figure S5**, Supporting Information), a 10 min waiting time was applied at each temperature to observe the equilibrium shape of the droplet. TEM images shown in **Figure 3(b)** show the interface of liquid eutectic metal seeds ($Au_{0.75}Ag_{0.25}$-Ge) containing equilibrium amounts of Ge and solid Ge nanowires of two

different diameters (23 and 65 nm) at different temperatures (440 and 480 ºC). Different liquid drop curvatures on nanowire sidewalls, *i.e.* different degrees of truncation of the contact line, were observed for the growth of varying diameter Ge nanowires from the $Au_{0.75}Ag_{0.25}$-Ge eutectic system (**Figure 3(b)**). Equilibrium wetting angles (θ) at the tri-junction varied with temperature and also with the radial dimension of the nanowires, for the Au-Ge (**Figure S6**) and different Au-Ag-Ge alloys (**Figure 3(b) and 4** for $Au_{0.75}Ag_{0.25}$-Ge system and $Au_{0.65}Ag_{0.35}$-Ge system respectively). For all of the eutectic systems studied, a pronounced wetting of the liquid drop, *i.e.* a decrease in the wetting angle (θ), into the nanowire sidewalls and a high degree of truncation of the TPB contact line was observed for thinner nanowires, whereas a much flatter growth front, with relatively small {113} facets at the corner of liquid-solid contact line was evident for thicker nanowires.

The balance of forces at the vapour-solid and liquid-solid interfaces determines the shape of the TPB. To satisfy the balance of forces along the vapour-solid surface, for a flatter growth front at the interface of the liquid drop and solid nanowire, γ_{vl} needs to be $\geq \gamma_{vs}$.[43] For the Au-Ge and Au-Ag-Ge systems, with a considerably high (> 25 at%) equilibrium Ge concentration in the metastable liquid melt, the liquid surface energy (γ_{vl}) decreases[35] as Ge incorporation into the seed lowers γ_{vl} and the surface force conditions for a flat growth front is rarely satisfied, resulting in a faceted triple junction at equilibrium. The amount of Ge in the liquid alloy at the nanowire tips is higher for the small diameter nanowires (**Figure 2(a)**). As a high content of Ge in the liquid eutectic alloy (Au-Ge and Au-Ag-Ge) lowers the liquid alloy's surface energy, a greater reduction in surface energy is expected for small diameter nanowires. Hence, the balance of forces at the liquid (seed)-solid (nanowire) junction drive the contact line towards prominent truncated structures for small diameter nanowires, with smaller wetting angles (θ) compared to large diameter nanowires.

Differences in the shape of the TPB are also observed with changes in the metal composition of the eutectics (Au, $Au_{0.75}Ag_{0.25}$ and $Au_{0.65}Ag_{0.35}$) for similar diameter nanowires (d = 68 nm) in-situ annealed at the same temperature (**Figure 5**). A large faceted growth front is observed with a pure Au-Ge system, whereas inclusion of Ag in the eutectic alloys forces the liquid-solid contact line towards a relatively flatter shape with smaller {113} corner facets. According to Young's balance of forces (surface forces) for a truncated TPB morphology, the net presence of an upward force at the liquid-solid interface is expected upon lowering the liquid-vapour surface energy.[43] The greater amount of Ge present in a Au-Ge eutectic liquid alloy compared to a Au-Ag-Ge eutectic of similar size (as inferred from the Ge-liquidus in **Figure 2(a)**) accounts for a smaller vapour-liquid surface energy (γ_{vl}) in Au-Ge compared in the Au-Ag-Ge alloys. For similar diameter nanowires, a greater imbalance in the Young's balance of forces at different interfaces with low γ_{vl} values for the Au-Ge system results in a faceted growth front, with higher facet curvature at the liquid-solid interface compared to Au-Ag-Ge system. The amount of Ag in the eutectic liquid alloy also plays a significant role in determining γ_{vl} of the eutectic liquid and hence wetting of the nanowire sidewalls.

2.3 Nanowire growth kinetics inferred from liquid seed-solid nanowire interfacial characteristics

The heterogeneous nature of the TPB facets has important implications for nanowire growth kinetics.[28] Forces present at the TPB, *i.e.* different surface energies, control the chemical potentials of the Ge facets and hence control the nucleation and growth kinetics.[23] The growth kinetics of the nanowires as a function of radial dimension and the metal composition of the seed, *i.e.* the relative amount of Au and Ag in the alloy, is expected to vary due to a change in the equilibrium Ge concentration (**Figure 2(a)**) in the eutectic melt.[14] For

different eutectics systems, *i.e.* Au-Ge and Au-Ag-Ge, of different dimensions and compositions, the differing amounts of Ge in the drop modifies the shape of the eutectic liquid alloy–solid nanowire interfaces for the equilibrated liquid drop-nanowire system, as discussed in the section above.

Different faceting behaviour with varying wetting angles (θ), during in-situ TEM annealing, is clearly evident for different diameter nanowires for all three eutectic systems studied (**Figure 3(b), 4 and S6**). The curvature and the length of the corner {113} facets at the liquid-solid contact vary as a function of metal composition (Au and Ag) in the alloy seed and nanowire diameter. An increase in the liquid contact area with the solid nanowire sidewall, and a decrease of the wetting angle, is obvious for the relatively small diameter nanowires with all three systems investigated. Considering three nanowires of similar diameters (~ 68 nm) grown from different eutectic systems (Au-Ge, $Au_{0.75}Ag_{0.25}$-Ge and $Au_{0.65}Ag_{0.35}$-Ge), increased faceting at the liquid-solid interface, *i.e.* increased area of the {113} side facets, was observed (**Figure 5**) to a greater extent for the binary Au-Ge system compared to the Au-Ag-Ge systems at 460 ºC (near our growth temperature). The growth rate of each facet, central {111} facet and corner {113} facets, during nanowire growth depends on the chemical potential difference of the growth species in the eutectic liquid and solid nanowire facets. The larger value of the chemical potential difference, *i.e.* higher supersaturation, means that the nucleation barrier for Ge crystallisation at the TPB is reduced, thus favouring faster nucleation and crystallisation of Ge growth species at the interface. The morphologies, *i.e.* the extension of the facet lengths (main growth facet and {113} side facets), of eutectic systems with different dimensions and compositions play an important role in revealing nanowire growth kinetics. Truncated {113} facets impact the interface nucleation and growth rates due to oscillatory nucleation/dissolution behaviour.[20] Clusters

13

of adatoms at the {113} facets lower the nucleation barrier and promote mass transfer towards the main growth facets, promoting nanowire growth along the [111] direction.[28] We can assume in our study that the shape of the heterogeneous interface at equilibrium, with the smaller side {113} facet lengths for systems with lower Ge equilibrium concentration (higher growth kinetics) encourages favourable growth along the main {111} growth facets, with faster/protracted oscillatory fluctuations of truncated facets during actual nanowire growth. In our post-growth in-situ experiments we are considering an immobile equilibrium growth picture (without any Ge flux) and are not observing time-resolved mobile liquid-solid interfacial behaviour for different nucleation cycles during steady state nanowire growth; which would be more conclusive evidence for the correlation of facet lengths with growth kinetics as reported by other researchers.[20, 21, 29, 30] Hence, for low equilibrium Ge concentration systems, *i.e.* ternary AuAg-Ge alloys, the geometry of the seed-nanowire interface changes towards a much flattened growth front (**Figure 5**) due to changes in the interfacial surface tensions and Wulff constructions, which in turn suggests faster growth kinetics with these systems. Theoretical estimations[23] also indicated a tendency for driving out the side facets for faster growth kinetics. Both classes of facets contribute towards the linear growth of nanowires. For nanowires with smaller extensions of truncated facets (at equilibrium), due to higher weighted curvature of relatively smaller facets, the chemical potential is higher at the smaller truncated facets. As growth velocity depends on the difference between the chemical potential of the growth species in a liquid catalyst and the solid facets, a higher chemical potential at smaller truncated facets decreases the growth velocity at side facets with a relatively higher growth rate at the main facets.

At equilibrium the liquid droplet at the tips of the nanowires has a uniform composition and chemical potential so that the balance of forces is in equilibrium to create a unique scalar

14

surface curvature of the liquid drop. The relatively flatter growth front, in an equilibrium state, with the large central {111} facet observed at 460 ºC for the eutectic system containing the highest amount of Ag (65 at.%), is due to lower Ge equilibrium concentration and reflects fast nanowire growth kinetics from $Au_{0.65}Ag_{0.35}$ seeds (**Figure 5**) compared to $Au_{0.75}Ag_{0.25}$ and Au seeds. Different curvatures of the liquid-solid interface and larger {113} side facets observed for the different diameter nanowires for all the eutectic systems studied (**Figure 3(b), 4 and S6** in Supporting Information) can be directly related to the Gibbs-Thompson effect, *i.e.* diameter dependent nanowire growth kinetics. Liquid-solid contact lines with longer side facet ({113}) lengths, were observed for thin nanowires compared to thick nanowires grown from a certain type of eutectic alloy drop, which is characteristic of eutectic systems with higher Ge equilibrium concentrations, *i.e.* with lower supersaturation and growth kinetics. So the Gibbs-Thompson effect for nanowire growth can be directly interpreted from the liquid-solid interfacial behaviour as the interface morphology is directly related to nanowire growth kinetics. The in-situ observation of the liquid-solid interfaces and the morphology of the nanowire growth front relate well with the reported theoretical simulations of the TPB behaviour in nanowire growth kinetics.[22, 23, 28] Also, the part the Ge equilibrium concentration (C_e) plays in determining the supersaturation and nanowire growth kinetics with the eutectic systems with different metal compositions is obvious from the fact that the eutectic liquid, having a lower Ge equilibrium content ($Au_{0.65}Ag_{0.35}$-Ge), displays relatively flattened interfacial curvature at the TPB, which correlates with faster nanowire growth kinetics. Diameter dependent ex-situ growth rate measurements (see Supporting Information for detail) for the synthesised Ge nanowires from different catalyst systems also depicted a faster growth rate for relatively thicker nanowires grown from Ag-rich seeds (**Figure S7**, Supporting Information), agreeing well with the findings from the TPB shape-based arguments for the nanowire growth kinetics. Larger diameter nanowires grown from

seeds with a high Ag content showed relatively flat growth fronts (**Figures 3, 4 and 5**) and exhibited fast growth kinetics, with a non-linear dependence on nanowire diameter.

2.4 Liquid seed-solid nanowire interfacial characteristics and nanowire diameter

Nanowire diameter is another important aspect to contemplate when considering the relative wettability and change in the volume of the liquid catalyst droplet at the tip of the nanowires, as a function of liquid-drop composition. Surface energies at different interfaces accordingly define the mean eutectic drop volume and nanowire diameter.[16, 45, 46] Nanowire diameter (d) relates to the catalyst drop volume (V), taking the growth front wetting into consideration, as $d = V^{1/3} f(\beta)$, where $f(\beta)$ is a function of the contact angle (β) of the droplet with the nanowire growth front.[32, 43] The growth of two different diameter nanowires from similar sized catalyst drops of different eutectic compositions correlates with different wetting behaviour of the liquid alloy and different surface energies at the growth front. As $f(\beta)$ changes for similar volume (V) catalyst drops of Au-Ge and Au-Ag-Ge, nanowires of different diameters are expected from different catalytic drops of similar size. One such example is shown in **Figure 6(a)**, where two different catalyst drops of similar volumes (1.19×10^{-4} μm^3 for $Au_{0.75}Ag_{0.25}$ -Ge and 1.17×10^{-4} μm^3 for Au-Ge) at 480 °C results in nanowires with different diameters. For the $Au_{0.75}Ag_{0.25}$ alloy seed the nanowire diameter is 47 nm whereas for the Au particle seed the nanowire diameter is 35 nm. As observed in **Figure 6(a)**, the different wetting and shapes of the nanoparticle drops at the tip of the nanowires leads to different nanowire diameters. Large wetting angles of liquid drops ($\beta = 140°$) for the $Au_{0.75}Ag_{0.25}$-Ge eutectic alloy results in nanowires with narrower radial dimensions compared to Au-Ge systems where the wetting angle is smaller ($\beta = 101°$). Plots showing a few examples of the variation in nanowire diameter with catalyst drop volume (a larger value of $f(\beta)$ signifies a smaller drop volume, as $f(\beta)$ correlates with d and V), for both the Au-Ge and $Au_{0.75}Ag_{0.25}$-Ge

16

systems, are shown in **Figure 6(b)**. The data clearly show the requirement for a larger eutectic catalyst Au-Ge drop compared to Au-Ag-Ge drop for the growth of similar diameter nanowires, especially in the narrower diameter range (< 50 nm). No clear trend in the behaviour of $f(\beta)$ as a function diameter (figure 6(b)) was observed, possibly due to the theoretical requirement for cylindrical cross sectioned nanowires to satisfy the relationship between d, V and $f(\beta)$.

3. Conclusion

In conclusion, the equilibrium concentration of Ge and Ge-liquidus projections were determined for different binary (Au-Ge) and ternary (Au-Ag-Ge) eutectic alloys using in-situ TEM heating experiments. The change in the equilibrium concentrations and supersaturation with different metal compositions in the alloys was related to the different eutectic liquid-solid nanowire interfacial behaviour. Furthermore, growth kinetics of the nanowires synthesised from different catalytic seeds was associated with the shape of the liquid-solid contact line in a steady state nanowire growth scenario. Varying compositions of the metal components in the alloy seeds facilitated manipulation of the Ge equilibrium concentration for different supersaturation. Ag-rich eutectic alloys showed relatively flattened liquid-solid interfaces which correlate with faster nanowire growth kinetics. The Gibbs-Thompson effect for the growth of Ge nanowires with binary and ternary eutectic systems was inferred from facet dynamics at the TPB, with thin nanowires showing liquid-solid interfacial characteristics of slower nanowire growth kinetics, with a higher degree of truncation and longer {113} side facets at the catalyst-nanowire interface. Evidence of the correlation between the equilibrium concentration, growth kinetics, and liquid metal-semiconductor interfacial behaviour exhibited here for VLS nanowire growth, could lead to surface engineering of the different interfaces for complex nanowire growth and defect engineering.

17

Keeping in mind the large amount of possible metal alloy combinations which can act as growth promoters for group 14 and 13-15 nanowires, ternary eutectic systems have the potential to introduce unlimited thermodynamic and energetic variation in the catalyst phase to greatly influence nanowire growth.

Supporting Information

Nanowire and seed nanoparticle synthesis detail and calculation of the equilibrium concentration of the alloy seeds at the tip of the nanowires, detail of the nanowires including growth direction, TEM images recorded at high temperatures to show the liquid-solid interfacial behavior for different catalyst system, nanowire growth rate. This material is available free of charge via Wiley Online Library.ch

Acknowledgements

References

[1] E. Garnett, P. D. Yang, *Nano Lett.* **2010**, *10*, 1082.

[2] F. Leonard, A. A. Talin, B. S. Swartzentruber, S. T. Picraux, *Physical review letters* **2009**, *102*, 106805.

[3] J. Xiang, W. Lu, Y. J. Hu, Y. Wu, H. Yan, C. M. Lieber, *Nature* **2006**, *441*, 489.

[4] K. S. Yi, K. Trivedi, H. C. Floresca, H. Yuk, W. Hu, M. J. Kim, *Nano Lett.* **2011**, *11*, 5465.

[5] A. M. Chockla, K. C. Klavetter, C. B. Mullins, B. A. Korgel, *Acs Applied Materials & Interfaces* **2012**, *4*, 4658.

[6] F. Shen, J. Wang, Z. Xu, Y. Wu, Q. Chen, X. Li, X. Jie, L. Li, M. Yao, X. Guo, T. Zhu, *Nano Lett.* **2012**, *12*, 3722.

[7] Y.-C. C. Liu, N. Rieben, L. Iversen, B. S. Sorensen, J. Park, J. Nygard, K. L. Martinez, *Nanotechnology* **2010**, *21*.

[8] J. Andzane, N. Petkov, A. I. Livshits, J. J. Boland, J. D. Holmes, D. Erts, *Nano Lett.* **2009**, *9*, 1824.

[9] E. I. Givargizov, *Journal of Crystal Growth* **1975**, *31*, 20.

[10] B Lewis, J. S. Anderson, *Nucleation and Growth of Thin Films*, Academic, New York, 1978.

[11] S. A. Dayeh, S. T. Picraux, *Nano Lett.* **2010**, *10*, 4032.

[12] R. E. Algra, M. A. Verheijen, L. F. Feiner, G. G. W. Immink, W. J. P. van Enckevort, E. Vlieg, E. Bakkers, *Nano Lett.* **2011**, *11*, 1259.

[13] P. L. A Prince, O Fabrichnaya, *Springer Materials The Landotl-Bornstein New Series IV/IIB*, Springer, 2012.

[14] S. Biswas, C. O'Regan, N. Petkov, M. A. Morris, J. D. Holmes, *Nano Lett.* **2013**, *13*, 4044.

[15] E. A. Sutter, P. W. Sutter, *ACS Nano* **2010**, *4*, 4943.

[16] E. Sutter, P. Sutter, *Nano Lett.* **2008**, *8*, 411.

[17] E. J. Schwalbach, P. W. Voorhees, *Nano Lett.* **2008**, *8*, 3739.

[18] T. Haxhimali, D. Buta, M. Asta, P. W. Voorhees, J. J. Hoyt, *Physical Review E* **2009**, *80*, 050601.

[19] S. Hofmann, R. Sharma, C. T. Wirth, F. Cervantes-Sodi, C. Ducati, T. Kasama, R. E. Dunin-Borkowski, J. Drucker, P. Bennett, J. Robertson, *Nature Materials* **2008**, *7*, 372.

[20] A. D. Gamalski, C. Ducati, S. Hofmann, *Journal of Physical Chemistry C* **2011**, *115*, 4413.

[21] C. Y. Wen, J. Tersoff, K. Hillerich, M. C. Reuter, J. H. Park, S. Kodambaka, E. A. Stach, F. M. Ross, *Physical review letters* **2011**, *107*, 025503.

[22] K. W. Schwarz, J. Tersoff, *Physical review letters* **2009**, *102*, 206101.

[23] K. W. Schwarz, J. Tersoff, *Nano Lett.* **2011**, *11*, 316.

[24] V. G. Dubrovskii, G. E. Cirlin, N. V. Sibirev, F. Jabeen, J. C. Harmand, P. Werner, *Nano Lett.* **2011**, *11*, 1247.

[25] G. Collins, M. Kolesnik, V. Krstic, J. D. Holmes, *Chem. Mat.* **2010**, *22*, 5235.

[26] T. Hanrath, B. A. Korgel, *Advanced Materials* **2003**, *15*, 437.

[27] M. Koto, A. F. Marshall, I. A. Goldthorpe, P. C. McIntyre, *Small* **2010**, *6*, 1032.

[28] H. Wang, L. A. Zepeda-Ruiz, G. H. Gilmer, M. Upmanyu, *Nature communications* **2013**, *4*, 1956.

[29] B. J. Kim, J. Tersoff, S. Kodambaka, M. C. Reuter, E. A. Stach, F. M. Ross, *Science* **2008**, *322*, 1070.

[30] C. Y. Wen, J. Tersoff, M. C. Reuter, E. A. Stach, F. M. Ross, *Physical review letters* **2010**, *105*, 195502.

[31] V. Schmidt, S. Senz, U. Goesele, *Physical Review B* **2007**, *75*, 045335.

[32] V. Schmidt, J. V. Wittemann, S. Senz, U. Goesele, *Advanced Materials* **2009**, *21*, 2681.

[33] V. G. Dubrovskii, N. V. Sibirev, *Physical Review E* **2004**, *70*, 031604.

[34] S. Kodambaka, J. Tersoff, M. C. Reuter, F. M. Ross, *Science* **2007**, *316*, 729.

[35] H. Adhikari, A. F. Marshall, I. A. Goldthorpe, C. E. D. Chidsey, P. C. McIntyre, *ACS Nano* **2007**, *1*, 415.

[36] V. Schmidt, J. V. Wittemann, U. Goesele, *Chemical Reviews* **2010**, *110*, 361.

[37] S. Barth, O. Kazakova, S. Estrade, R. G. Hobbs, F. Peiro, M. A. Morris, J. D. Holmes, *Crystal Growth & Design* **2011**, *11*, 5253.

[38] C. O'Regan, S. Biswas, C. O'Kelly, S. J. Jung, J. J. Boland, N. Petkov, J. D. Holmes, *Chem. Mat.* **2013**, *25*, 3096.

[39] H. Geaney, E. Mullane, K. M. Ryan, *Journal of Materials Chemistry C* **2013**, *1*, 4996.

[40] N. Han, F. Wang, J. J. Hou, S. P. Yip, H. Lin, M. Fang, F. Xiu, X. Shi, T. F. Hung, J. C. Ho, *Cryst. Growth. Des.* **2012**, *12* 6243.

[41] B. A. Wacaser, K. A. Dick, J. Johansson, M. T. Borgstrom, K. Deppert, L. Samuelson, *Advanced Materials* **2009**, *21*, 153.

[42] J. Wallentin, M. Ek, L. R. Wallenberg, L. Samuelson, K. Deppert, M. T. Borgstrom, *Nano Lett.* **2010**, *10*, 4807.

[43] S. Crawford, S. K. Lim, S. Gradecak, *Nano Lett.* **2013**, *13*, 226.

[44] A. A. Stekolnikov, F. Bechstedt, *Physical Review B* **2005**, *72*, 125326.

[45] Y. Cui, L. J. Lauhon, M. S. Gudiksen, J. F. Wang, C. M. Lieber, *Applied Physics Letters* **2001**, *78*, 2214.

[46] B. Eisenhawer, V. Sivakov, S. Christiansen, F. Falk, *Nano Lett.* **2013**, *13*, 873.
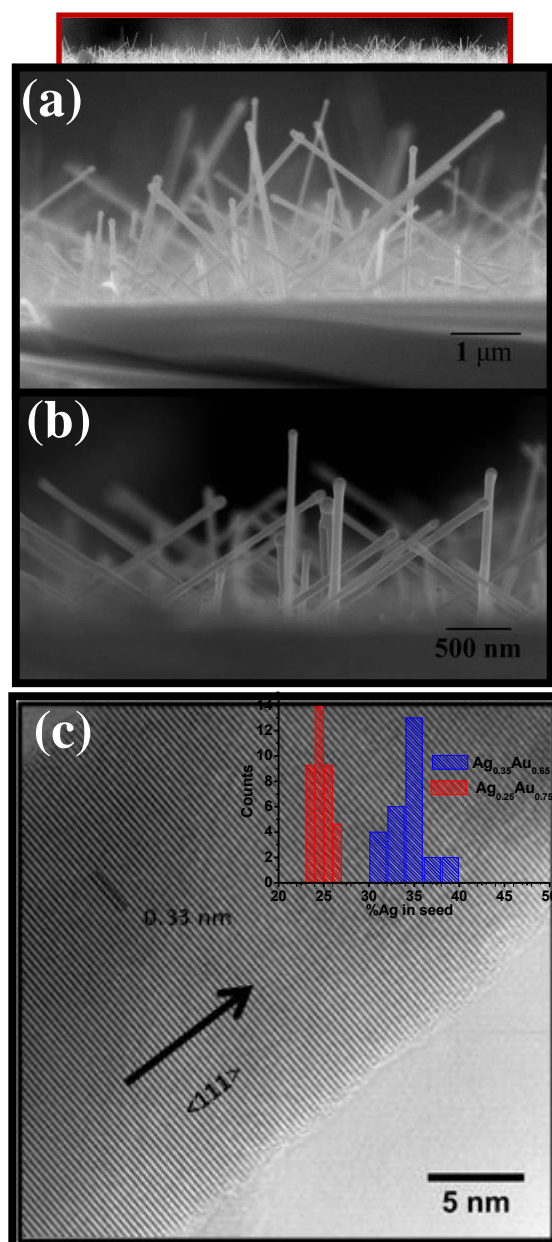
Figure 1. SEM images of Ge nanowire synthesised from: (a) a $Au_{0.75}Ag_{0.25}$ catalyst and (b) a Au catalyst on Ge (001) substrates after a 45 min growth time. Part (b) shows a TEM image of (111)-directed Ge-nanowire. Insets in part (b) depicts the composition of Ag in the droplet seed (estimated from EDX) for two alloy systems at room temperature.
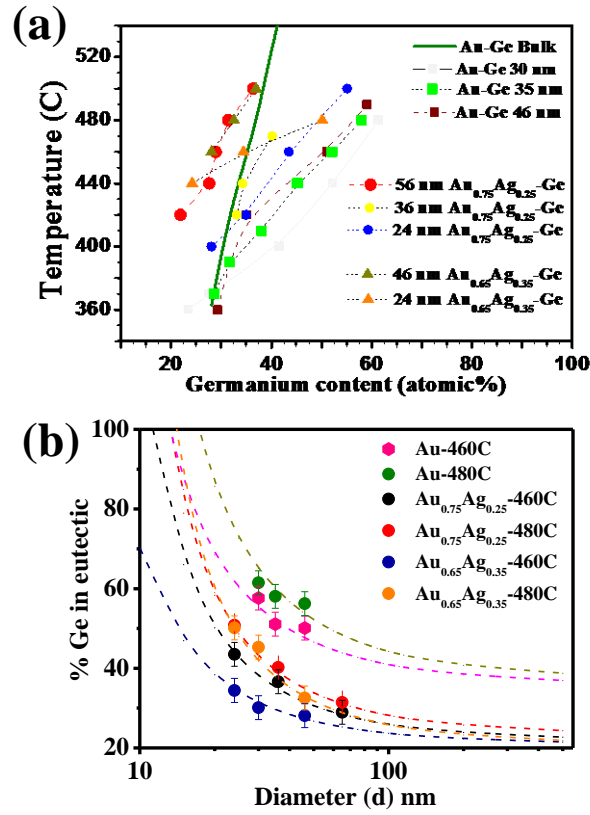
Figure 2. (a) Ge-liquidus curves showing the shift in the atomic concentration of Ge with different ratios of Au and Ag in the eutectic alloys. Prominent nanoscale effect for all three eutectic systems is evident from the plot. (b) Theoretical fit (dashed lines) according to the Gibbs-Thompson effect and experimental data for all three Ge-eutectic compositions at different radial dimensions.
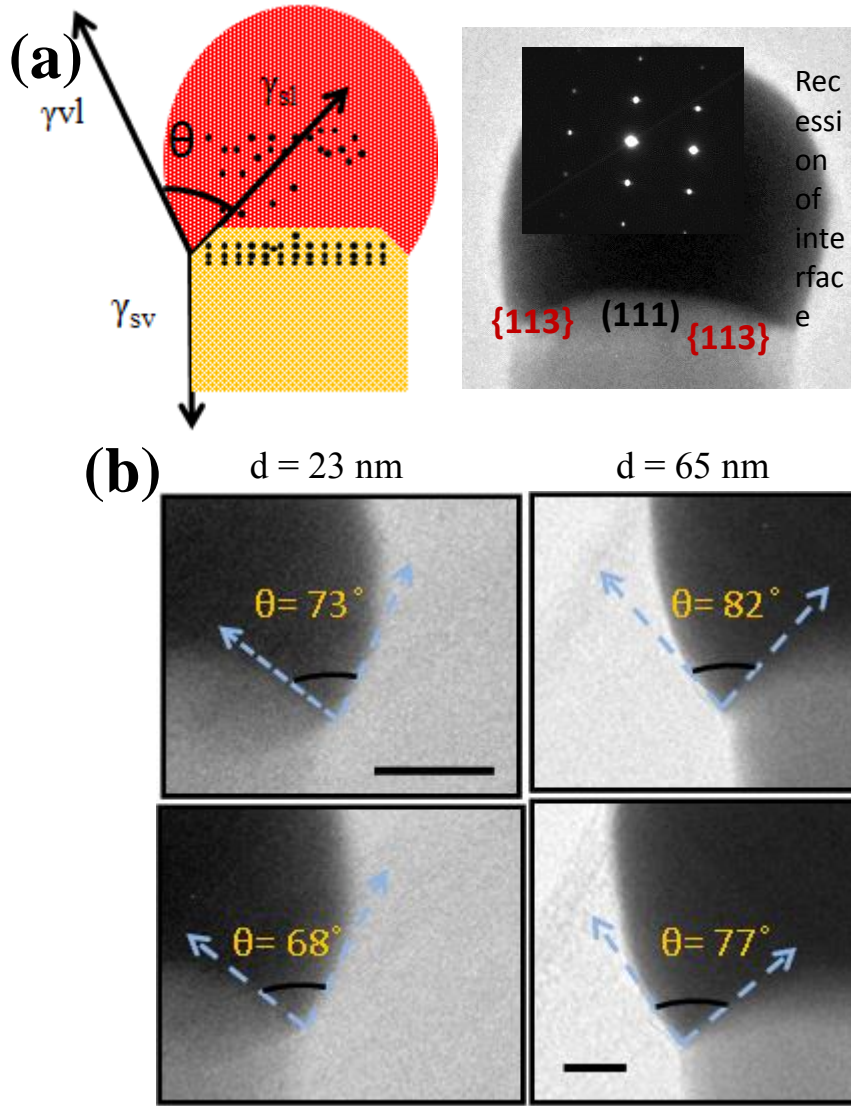
Figure 3. (a) Schematic of a liquid drop-nanowire interface and a TEM image of a Au-Ge eutectic and Ge nanowire interface. The inset shows an SAED of the liquid catalyst-solid nanowire interface. (b) TEM images showing eutectic liquid-solid nanowire interfaces for two different diameter nanowires; 23 nm and 65 nm. Different wetting of the liquid eutectic ($Au_{0.75}Ag_{0.25}$-Ge eutectic) was evident at different temperatures from the different contact angles between eutectic droplet and nanowire side walls. Different facet length scales at the liquid-solid interface advocate diameter dependent growth. Scale bar denotes 10 nm.
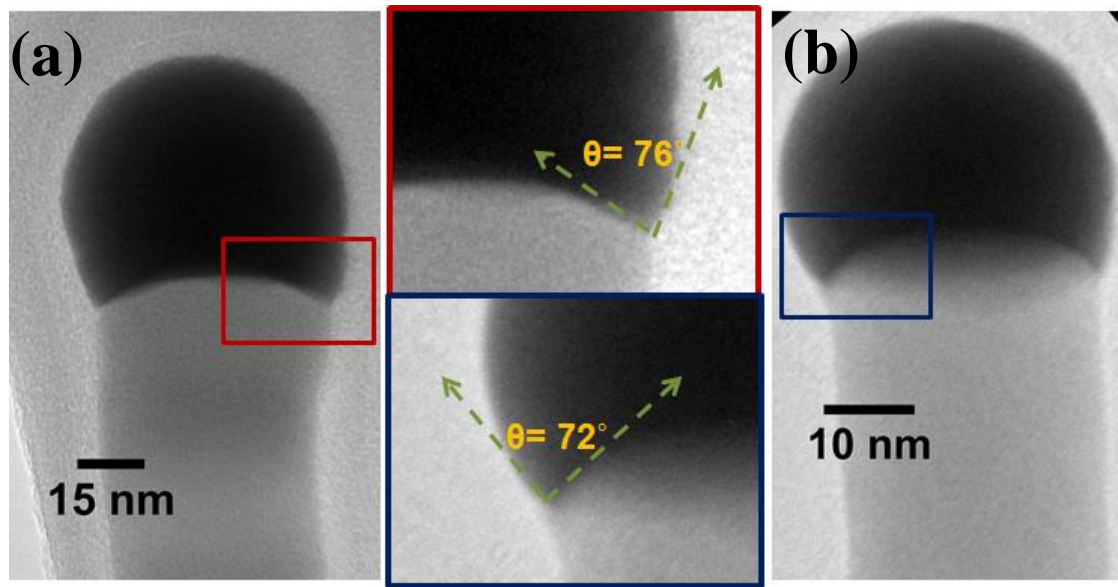
Figure 4. TEM images showing liquid catalyst-solid nanowire interfacial behavior for Au$_{0.65}$Ag$_{0.35}$-Ge system. Gibbs-Thompson effect (diameter dependent growth) in nanowire growth was evident from the behavior of the contact angles of eutectic liquid droplets with side wall facets of nanowire for different diameter nanowires with Au-Ag-Ge alloy: (a) 47 nm and (b) 30 nm. Liquid-solid interface is expanded in the insets with corresponding color index.
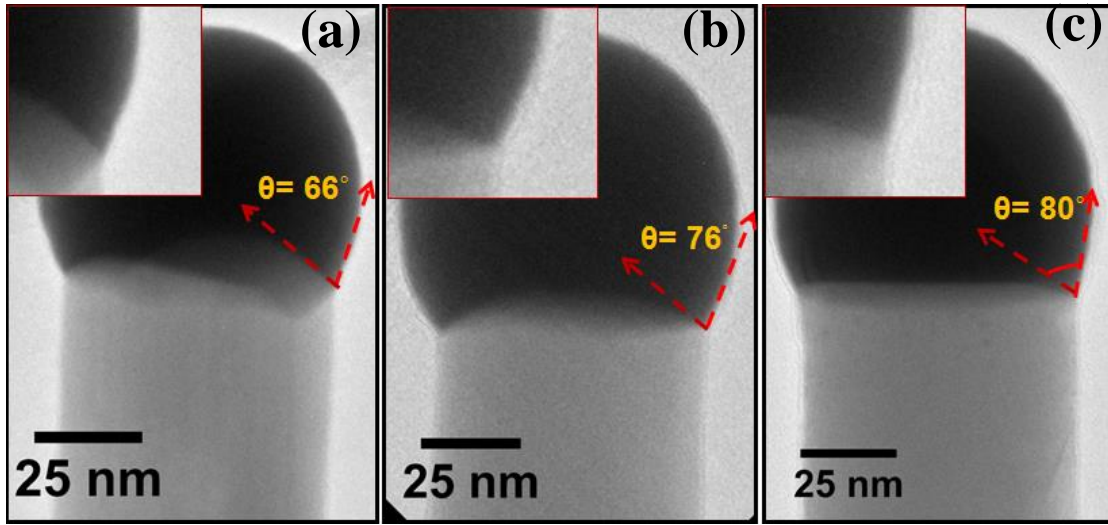
Figure 5. Participation of different nanowire growth kinetics for different eutectic alloys with same diameter (68 nm) nanowire; (a) Au-Ge, (b) $Au_{0.75}Ag_{0.25}$ and (c) $Au_{0.65}Ag_{0.35}$, was evident from different contact angles of eutectic drop with nanowire side facets from the TEM images recorded at 460 ℃.
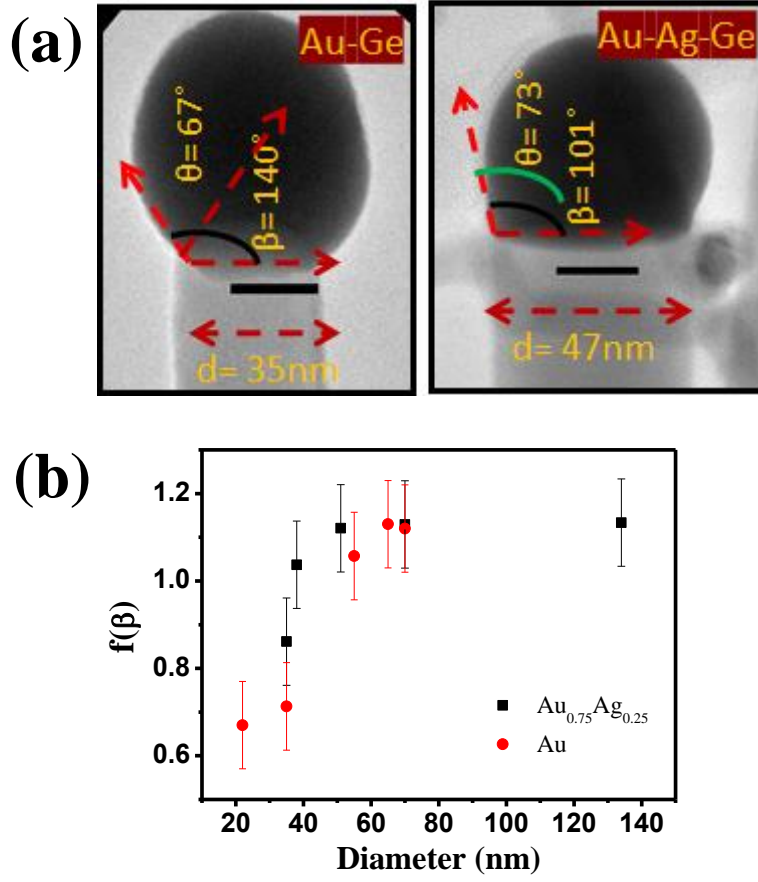
Figure 6. (a) TEM images shows two different eutectic systems of similar volume resulted in different nanowire diameters. Differences in the wetting behavior of the liquid catalyst for Au-Ge and Au-Ag-Ge are also evident from the TEM images (scale bar depicts 20 nm length). (b) Variation in liquid drop wetting behavior (*f(β)*) with nanowires of different diameters for Au-Ge and Au-Ag-Ge eutectic systems.

TOC text:

In-situ Transmission electron microscopy (TEM) at elevated temperature is used to observe the characteristics of ternary (Au-Ag-Ge) liquid eutectic catalyst drop and nanowire interfaces at nanowire growth temperature. At high temperature germanium equilibrium concentrations in the eutectic melts determine the geometry of the heterogeneous nanowire-catalyst interface which is correlated with the diameter and eutectic composition dependent nanowire growth kinetics.

Subhajit Biswas, Colm O'Regan, Michael A. Morri, and Justin D. Holmes [*]

Title

In-situ Observations of Nanoscale Effects in Germanium Nanowire Growth with Ternary Eutectic Alloys

TOC Graphic:
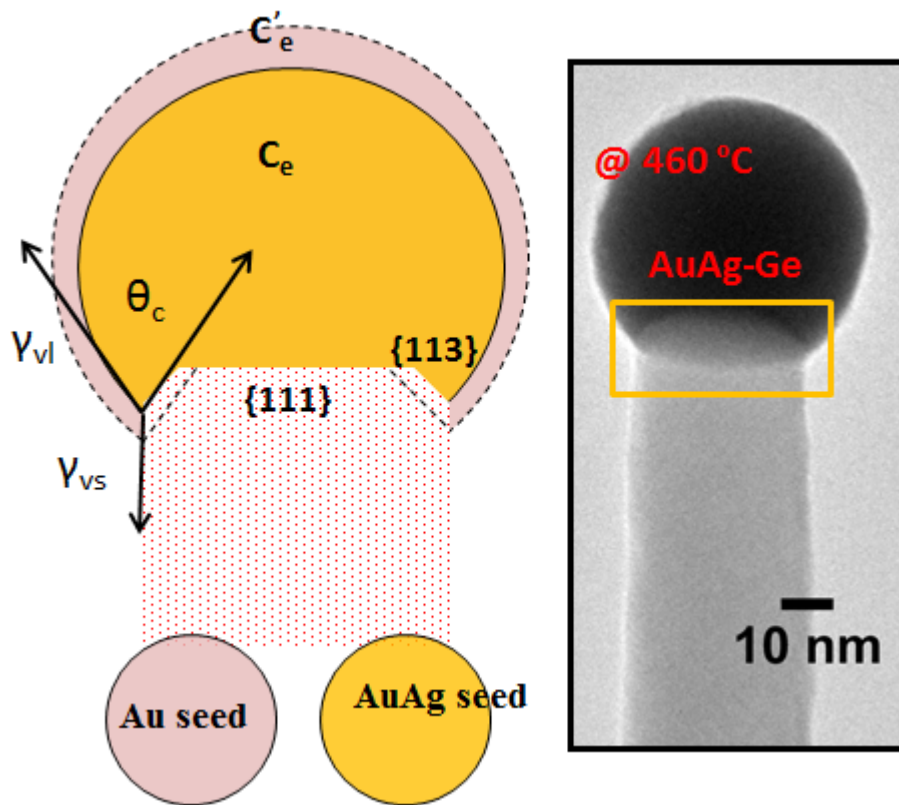
Supporting Information

In-situ Observations of Nanoscale Effects in Germanium Nanowire Growth with Ternary Eutectic Alloys

Subhajit Biswas, Colm O'Regan, Michael A. Morri, and Justin D. Holmes [*]

Materials Chemistry & Analysis Group, Department of Chemistry and the Tyndall National Institute, University College Cork, Cork, Ireland. Centre for Research on Adaptive Nanostructures and Nanodevices (CRANN), Trinity College Dublin, Dublin 2, Ireland.

Experimental Methods:

Nanoparticle synthesis: A colloidal dispersion of seed nanoparticles with different Au and Ag ratios were synthesized by varying the molarity of the Au^+ and Ag^+. Dodecanethiol (DDT)-stabilized nanoparticles were prepared in chloroform using tetra-octyel amino bromide (TOAB), $(C_8H_{17})_4NBr$, as a phase transfer catalyst and an aqueous sodium borohydride solution (~0.44 M), $NaBH_4$, as the reducing agent. The organic phase was separated and precipitated with ethanol. The precipitation was cleaned with ethanol and redispersed in toluene for further use as catalyst in nanowire growth.

Nanowire synthesis: Continuous-flow reactions for nanowire growth were carried out in a toluene medium using a liquid-injection chemical vapor deposition (LICVD) technique. Metal nanoparticles were spin-coated onto a H-terminated Si (001) or Ge (001) substrate and loaded into a stainless steel micro reactor cell, connected to metal tubing. The reaction cell and connections were dried for 24 hr at 180 ℃ under vacuum. Solutions of diphenylgermane (DPG), the Ge precursor, in anhydrous toluene were prepared in an N_2 glove box with a typical concentration of 5 μmole ml^{-1}. A DPG solution (5 μmole ml^{-1}) was loaded into a Hamilton sample-lock syringe inside a nitrogen-filled glovebox. Prior to injection, the coated Si substrate was annealed for 15 min at 460 ℃ under a flowing H_2/Ar atmosphere inside a tube furnace. The precursor solution was then injected into the metal reaction cell using a high pressure syringe pump at a rate of 0.025 ml min^{-1}. A H_2/Ar flow rate of 0.5 ml min^{-1} was maintained during the entire growth period. Typical growth times were varied to study the effect on nanowire length. The reaction cell was allowed to cool to room temperature and disassembled to access the growth substrate. Nanowires were washed with dry toluene and dried under N_2 flow for further characterization.
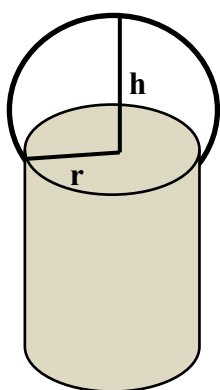
Characterization: The one-dimensional Ge nanostructures were analyzed using a FEI quanta 650 scanning electron microscope (SEM) and a JEOL 2100 transmission electron microscope (TEM) operated at 200 kV equipped with an EDX detector (Oxford Instruments INCA energy system). X-ray diffraction (XRD) studies were performed on a Phillips Xpert diffractometer. The TEM heating experiments were performed on a JEOL 2100 TEM equipped with a Gatan 652 high-temperature sample holder. The in-situ experiments cover the temperature range from room temperature to 500 ℃.

Measurement of equilibrium concentration: Equilibrium concentrations was measured by heating the nanowires deposited on lacey carbon coated Cu grids (3 mm diameter). In-situ experiments cover the temperature range between room temperature and 500 ºC. The electron beam intensity was kept low (~ 1 A/ cm^2) during the in-situ observation. To avoid any change in the thermal environment between different nanowires during a single heating experiment nanowires in close proximities (in a 10×10 μm^2 area) were considered. Alloy compositions in the eutectic seeds at the tips of the nanowires at high temperatures were measured from the expansion of volume (*V(T)-V(RT)*) of the catalyst drop from room temperature to high temperature. The equilibrium Ge content was calculated according to $N_{Ge} = (V(T) - V(RT)/v_{Ge}$, where N_{Ge} is the number of Ge atoms in the drop and v_{Ge} are atomic volumes of germanium (calculated from atomic mass and density). Atomic percentage (X_{Ge}) of Ge content in the eutectic was calculated according to $X_{Ge} = (N_{Ge}/(N_{AuAg} + N_{Ge})) \times 100$ where N_{AuAg}, number of Au and Ag atoms in the drop was calculated from the room temperature volume according to $N_{AuAg} = V(RT)/v_{AuAg}$, where v_{AuAg} is the atomic volume of Au-Ag alloy. We have considered the catalyst shape at the tip of the nanowire as spherical cap and volume (*V*) at room temperature and high temperature was calculated according to $V= \pi h/6 \ (3r^2 + h^2)$, where *r* is the radius of the cap and *h* is the height (see figure attached with this section). A five percent error was incorporated in the calculation of equilibrium concentrations (**Figure 2(b)**) to consider the deviation of the shape from the exact spherical cap.

Measurement of contact angle: Contact angles were measured at the liquid catalyst seed and solid nanowire interface by using imageJ and digitalmicrograph software. High-resolution TEM images were used to precisely measure the angle at the tri-junction. Results obtained with both the software were compared to minimise the error in the angle measurement. An

31

approximate random error of ± 2° is present due to manual error and Fresnel fringe contrast.

The lines drawn in the TEM images to reflect the angles serve as guide to the eye.

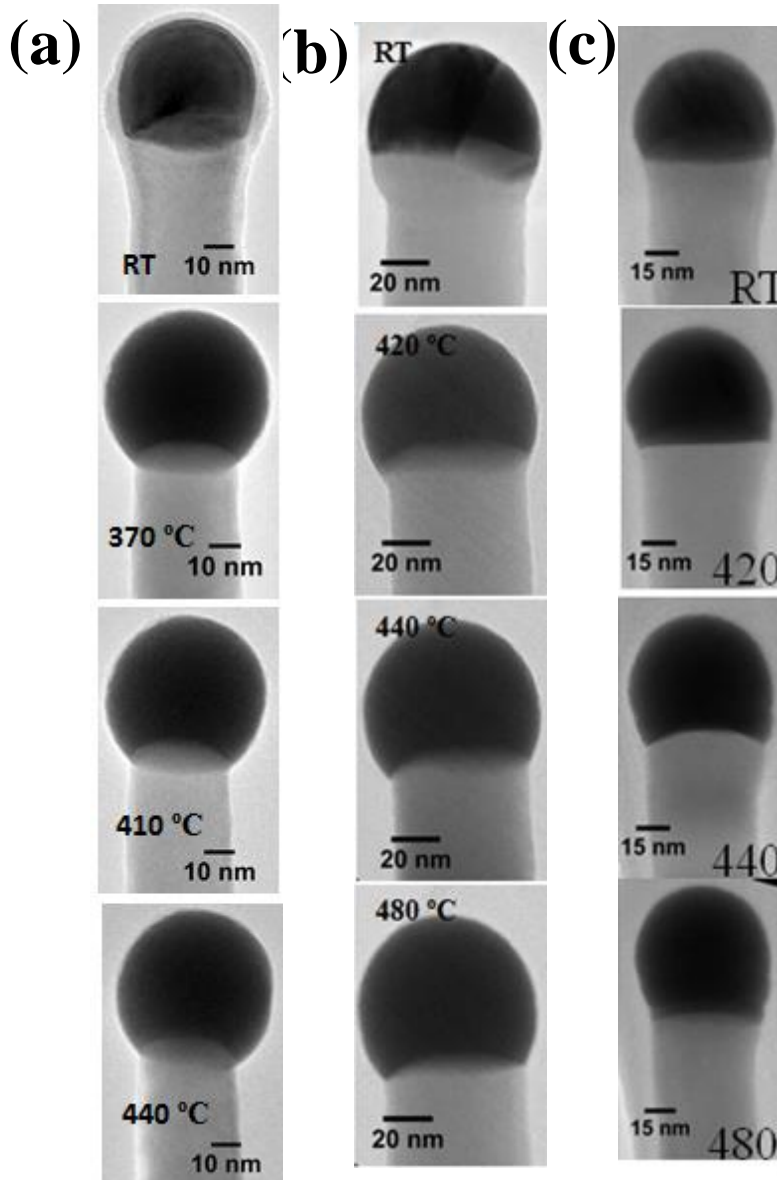**Figure S1**. Melting for three different eutectic systems: (a) 38 nm Au-Ge (b) 46 nm $Au_{0.75}Ag_{0.25}$-Ge and (c) 46 nm $Au_{0.65}Ag_{0.35}$-Ge is shown through TEM images during in-situ annealing of metal droplets at the tip of the nanowires between room temperature and 480 °C.
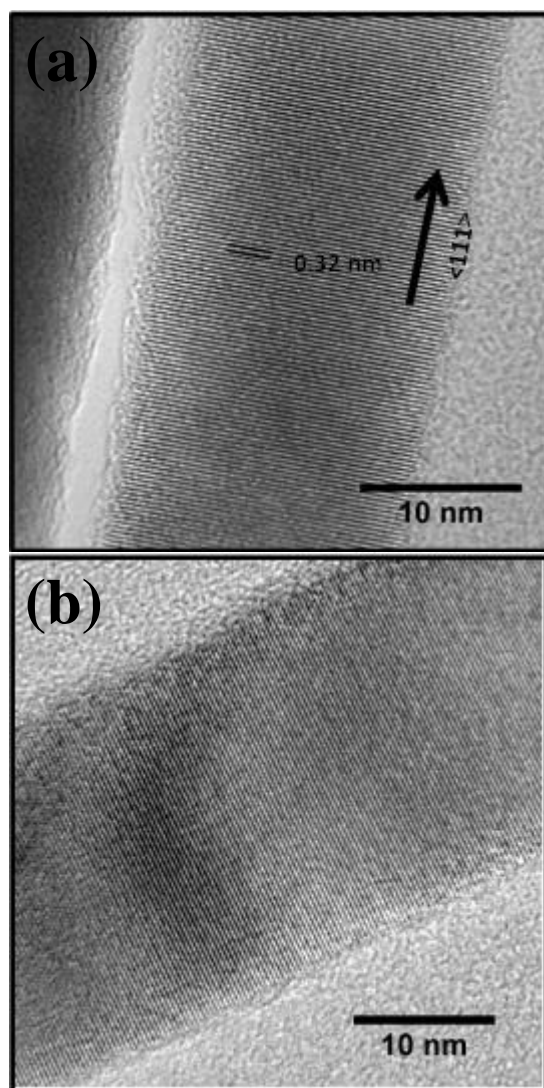
Figure. S2. (a-b) TEM images showing a few examples of (111)-directed Ge-nanowires.

SAED patterns From tip area
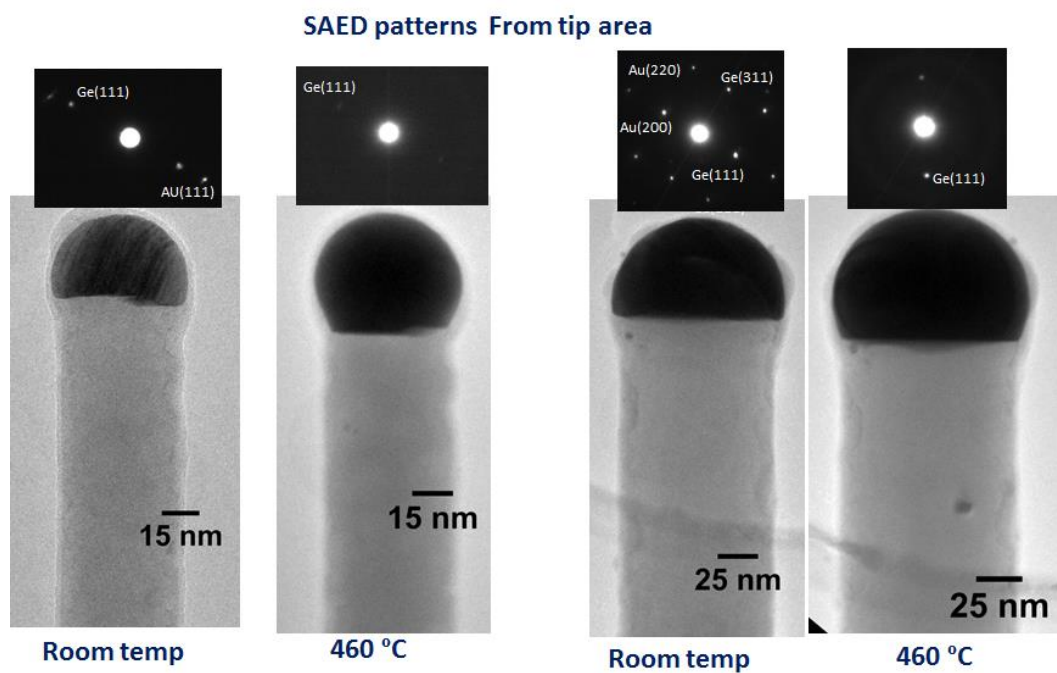
Figure S3. Eutectic melting is observed for $Au_{0.65}Ag_{0.35}$-Ge systems of two different dimensions (left: 45 nm and right: 95 nm) as confirmed from the SAED pattern in the inset. No diffraction spots corresponding to metal components are observed at high temperature.
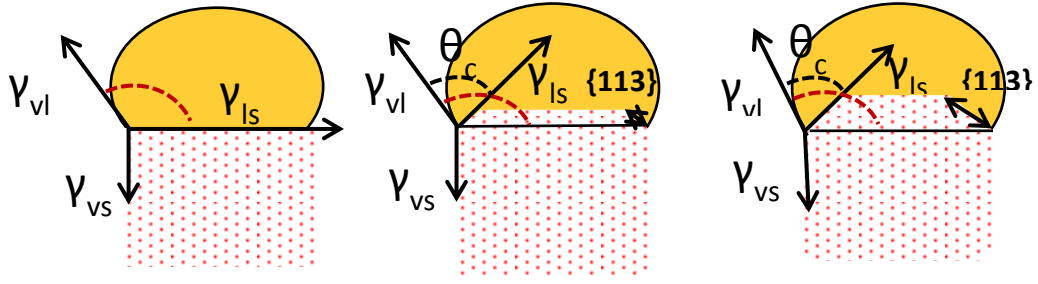
Figure S4. Schematic showing morphologies at the triple phase boundary with: (a) flat growth from and (b, c) faceted growth front with different degree of truncation, *i.e.* the length of {113} facets. Arrows show different interfacial surface forces.
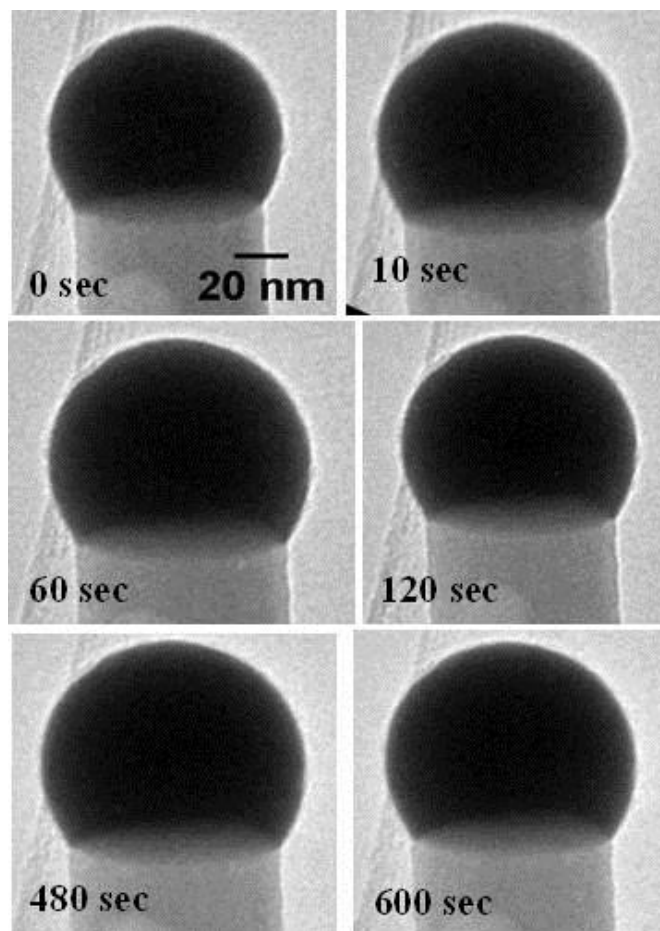
Figure S5. TEM images showing the time dependent change in the eutectic $Au_{0.75}Ag_{0.25}$-Ge droplet shape at 460 ℃; a stable equilibrium structure was formed after a 8-10 min interval.
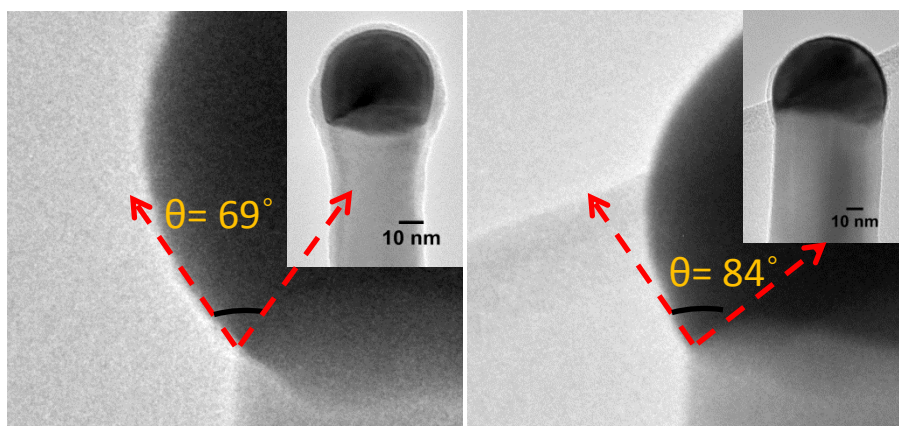
Figure S6. The Gibbs-Thompson effect on nanowire growth was also evident from the TEM images for Au-Ge eutectics from the behavior of the contact angles of eutectic liquid droplets (at 460 ºC) with side wall facets of nanowire for different diameter nanowires: (a) 36 nm and (b) 70 nm.
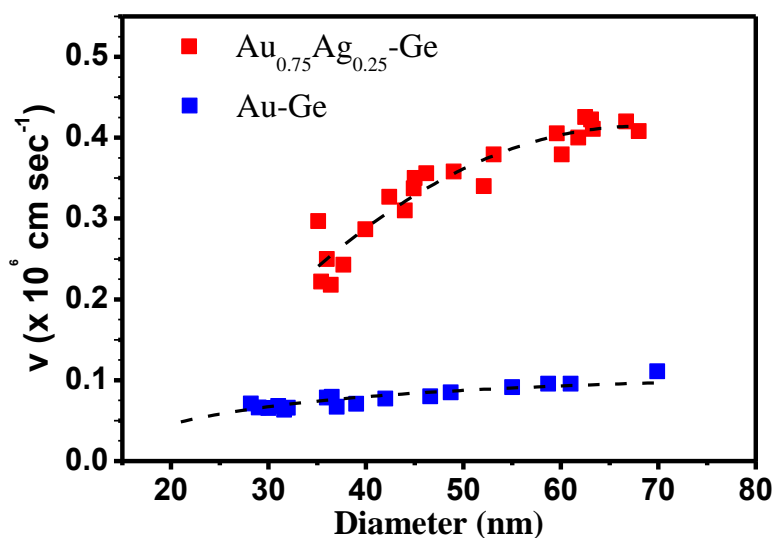
Figure S7. Graph showing the non-linear dependence of the nanowire growth rate with nanowire diameter for two different seeds. The ternary seed enables a higher growth velocity compared to pure Au seeds. The length of the nanowires were measured by dark-field STEM, after transferring the nanowires from growth substrate to a SiN membrane grid. For the ex-situ growth rate measurements short length nanowires of shorter lengths (<10 μm) grown after 45 min growth time was used (unclear what you mean by this sentence – please clarify).